

# Core polarization effects on $C4$ form factors of $sd$ -shell nuclei

R.A. Radhi<sup>a</sup>

Department of Physics, College of Science, University of Baghdad, Baghdad, Iraq

Received: 24 January 2002 / Revised version: 18 May 2002 /

Published online: 6 March 2003 – © Società Italiana di Fisica / Springer-Verlag 2003

Communicated by P. Schuck

**Abstract.** Coulomb form factors of  $C4$  transitions in even-even  $N = Z$   $sd$ -shell nuclei ( $^{20}\text{Ne}$ ,  $^{24}\text{Mg}$ ,  $^{28}\text{Si}$  and  $^{32}\text{S}$ ) are discussed taking into account higher-energy configurations outside the  $sd$ -shell model space which are called core polarization effects. Higher configurations are taken into account through a microscopic theory, which allows particle-hole excitations from the  $1s$  and  $1p$  shells core orbits and also from the  $2s1d$ -shell orbits to the higher allowed orbits with excitations up to  $4\hbar\omega$ . The effect of core polarization is found essential in both the transition strengths and momentum transfer dependence of form factors, and gives a remarkably good agreement with the measured data with no adjustable parameters. The calculations are based on the Wildenthal interaction for the  $sd$ -shell model space and on the modified surface delta interaction (MSDI) for the core polarization effects.

**PACS.** 25.30.Dh Inelastic electron scattering to specific states – 21.60.Cs Shell model – 27.30.+t  $20 \leq A \leq 38$

## Introduction

Comparisons between calculated and measured longitudinal electron scattering form factors have long been used as stringent tests of models of nuclear structure. Shell model within a restricted model space succeeded in describing static properties of nuclei, when effective charges are used. The Coulomb form factors have been discussed for the stable  $sd$ -shell nuclei using  $sd$ -shell wave functions with phenomenological effective charges [1]. The model space wave functions defined by the orbits in the  $sd$ -shell region cannot describe the photon point data and the electron scattering form factors for the non-zero momentum transfer ( $q$ ) values without introducing effective charges. However, the introduction of effective charges may bring the calculated transition strengths, which are defined at the photon point, closer to the measured values, but the non-zero momentum transfer values might deviate appreciably from the measured values. A microscopic model has been proposed [2] to include effects from outside the model space, which is called core polarization effects. Coulomb form factors of  $E4$  transitions in the  $sd$ -shell nuclei were discussed taking into account core polarization effects using self-consistent Hartree-Fock + random phase approximation calculations, which gave a good agreement with experimental form factors [2]. The effect of core polarization was found to be essential [3] in describing the form factors of  $^{12}\text{C}$  and  $^{13}\text{C}$ . The first-order

core polarization effects were incorporated with the  $p$ -shell wave functions by Sato *et al.* [4], where the effects greatly improved the agreement with the experimental data. Restricted  $1p$ -shell models were found [5] to give just 45% of the total observed  $C2$  transition strength for  $^{10}\text{B}$  and only a 10% improvement was realized by expanding the shell model space to include  $2\hbar\omega$  configurations. The inclusion of even higher-excited configuration by means of core polarization calculation [5] was essential to remove the remaining short fall. First-order core polarization effects were studied in pion single-charge exchange reactions on  $^{15}\text{N}$  and  $^{13}\text{C}$  [6], where the cross-section were moderately affected by core polarization.

In the present work, the  $C4$  Coulomb form factors are studied for the even-even  $N = Z$  nuclei ( $^{20}\text{Ne}$ ,  $^{24}\text{Mg}$ ,  $^{28}\text{Si}$  and  $^{32}\text{S}$ ), in the framework of the  $sd$ -shell model. We include higher-energy configurations as a first-order core polarization. Transitions from the core  $1s$  and  $1p$  orbits and also from the  $2s1d$ -shell orbits to all the higher allowed orbits with excitations up to  $4\hbar\omega$  are taking into account. In the present analysis, we do not introduce any state-dependent parameters such as effective charges, which were introduced in the previous investigation of electron scattering form factors in this region. For the  $sd$ -shell model space wave functions, we adopt the interaction of Wildenthal [7]. For the core polarization calculations, the modified surface delta interaction (MSDI) [8] is used as a residual interaction. The single-particle wave functions are those of the harmonic-oscillator (HO) potential with

<sup>a</sup> e-mail: baguniv@uruklink.net

size parameter  $b = 1.869$  fm for  $^{20}\text{Ne}$ ,  $b = 1.813$  fm for  $^{24}\text{Mg}$ ,  $b = 1.827$  fm for  $^{28}\text{Si}$  and  $b = 1.881$  fm for  $^{32}\text{S}$  so as to reproduce the root mean square (rms) charge radii of these nuclei [1].

## Theory

The core polarization effect on the form factors is based on a microscopic theory, which combines shell model wave functions and configurations with higher energy as first-order perturbations; these are called core polarization effects. The reduced matrix elements of the electron scattering operator  $T_\Lambda$  is expressed in terms of the residual interaction  $V_{\text{res}}$  as follows:

$$\langle \Gamma_f || \hat{T}_\Lambda || \Gamma_i \rangle = \langle \Gamma_f || \hat{T}_\Lambda || \Gamma_i \rangle_{\text{MS}} + \langle \Gamma_f || \delta \hat{T}_\Lambda || \Gamma_i \rangle_{\text{HC}}, \quad (1)$$

where the states  $|\Gamma_i\rangle$  and  $|\Gamma_f\rangle$  are described by the model space wave functions. Greek symbols are used to denote quantum numbers in coordinate space and isospace, *i.e.*  $\Gamma_i \equiv J_i T_i$ ,  $\Gamma_f \equiv J_f T_f$  and  $\Lambda \equiv J T$ .

The model space (MS) matrix element is expressed as the sum of the product of the elements of the one-body density matrix (OBDM)  $\chi_{\Gamma_f \Gamma_i}^A(\alpha, \beta)$  times the single-particle matrix elements, and is given by [1]

$$\langle \Gamma_f || T_\Lambda || \Gamma_i \rangle_{\text{MS}} = \sum_{\alpha, \beta} \chi_{\Gamma_f \Gamma_i}^A(\alpha, \beta) \langle \alpha || T_\Lambda || \beta \rangle, \quad (2)$$

where  $\alpha$  and  $\beta$  label single-particle states (isospin is included) for the model space.

Similarly, the higher-energy configurations (HC) matrix element is written as

$$\langle \Gamma_f || \delta \hat{T}_\Lambda || \Gamma_i \rangle_{\text{HC}} = \sum_{\alpha, \beta} \chi_{\Gamma_f \Gamma_i}^A(\alpha, \beta) \langle \alpha || \delta \hat{T}_\Lambda || \beta \rangle. \quad (3)$$

According to the first-order perturbation theory, the higher-energy configurations single-particle matrix element is given by [8]

$$\begin{aligned} \langle \alpha || \delta \hat{T}_\Lambda || \beta \rangle &= \langle \alpha || \hat{T}_\Lambda \frac{Q}{E_i - H_0} V_{\text{res}} || \beta \rangle \\ &+ \langle \alpha || V_{\text{res}} \frac{Q}{E_f - H_0} \hat{T}_\Lambda || \beta \rangle. \end{aligned} \quad (4)$$

The operator  $Q$  is the projection operator onto the space outside the model space. For the residual interaction,  $V_{\text{res}}$ , we adopt the MSDI [8].  $E_i$  and  $E_f$  are the energies of the initial and final states, respectively. Equation (4) is written as [8]

$$\begin{aligned} \langle \alpha || \delta T_\Lambda || \beta \rangle &= \sum_{\alpha_1 \alpha_2 \Gamma} \frac{(-1)^{\beta + \alpha_2 + \Gamma}}{e_\beta - e_\alpha - e_{\alpha_1} + e_{\alpha_2}} (2\Gamma + 1) \\ &\times \left\{ \begin{array}{ccc} \alpha & \beta & \Lambda \\ \alpha_2 & \alpha_1 & \Gamma \end{array} \right\} \sqrt{(1 + \delta_{\alpha_1 \alpha})(1 + \delta_{\alpha_2 \beta})} \\ &\times \langle \alpha \alpha_1 | V_{\text{res}} | \beta \alpha_2 \rangle_\Gamma \langle \alpha_2 || T_\Lambda || \alpha_1 \rangle \\ &+ \text{terms with } \alpha_1 \text{ and } \alpha_2 \text{ exchanged with} \\ &\text{an overall minus sign,} \end{aligned} \quad (5)$$

where the index  $\alpha_1$  runs over particle states and  $\alpha_2$  over hole states and  $e$  is the single-particle energy. The core polarization parts are calculated allowing particle-hole excitations from the  $1s$ -,  $1p$ - and  $2s1d$ -shell orbits into higher orbits. These excitations are taken up to  $4\hbar\omega$ .

The single-particle matrix element reduced in both spin and isospin, is written in terms of the single-particle matrix element reduced in spin only [8]

$$\langle \alpha_2 || T_\Lambda || \alpha_1 \rangle = \sqrt{\frac{2T+1}{2}} \sum_{t_z} I_T(t_z) \langle \alpha_2 || T_{J t_z} || \alpha_1 \rangle \quad (6)$$

with

$$I_T(t_z) = \begin{cases} 1, & \text{for } T = 0, \\ (-1)^{1/2 - t_z}, & \text{for } T = 1, \end{cases} \quad (7)$$

where  $t_z = 1/2$  for a proton and  $-1/2$  for a neutron.

The reduced single-particle matrix element of the Coulomb operator is given by [9]

$$\begin{aligned} \langle \alpha_2 || T_\Lambda || \alpha_1 \rangle &= \int_0^\infty dr r^2 j_J(qr) \\ &\times \langle \alpha_2 || Y_J || \alpha_1 \rangle R_{n_1 \ell_1}(r) R_{n_2 \ell_2}(r), \end{aligned} \quad (8)$$

where  $j_J(qr)$  is the spherical Bessel function and  $R_{n\ell}(r)$  is the single-particle radial wave function.

Electron scattering form factor involving angular momentum  $J$  and momentum transfer  $q$ , between the initial and final nuclear shell model states of spin  $J_{i,f}$  and isospin  $T_{i,f}$  are [10]

$$\begin{aligned} |F_J(q)|^2 &= \frac{4\pi}{Z^2(2J_i + 1)} \left| \sum_{T=0,1} \begin{pmatrix} T_f & T & T_i \\ -T_z & 0 & T_z \end{pmatrix} \right|^2 \\ &\times \langle J_f T_f || T_{JT} || J_i T_i \rangle \left| F_{\text{cm}}^2(q) F_{\text{fs}}^2(q) \right|^2, \end{aligned} \quad (9)$$

where  $T_z$  is the projection of the initial and final states and is given by  $T_z = (Z - N)/2$ . The nucleon finite-size (fs) form factor is  $F_{\text{fs}}(q) = \exp(-0.43q^2/4)$  and  $F_{\text{cm}}(q) = \exp(q^2 b^2/4A)$  is the correction for the lack of translational invariance in the shell model.  $A$  is the mass number, and  $b$  is the harmonic-oscillator size parameter.

The single-particle energies are calculated according to [8]

$$\begin{aligned} e_{nlj} &= (2n + l - 1/2)\hbar\omega \\ &+ \begin{cases} -\frac{1}{2}(l+1)\langle f(r) \rangle_{nl}, & \text{for } j = l - 1/2, \\ \frac{1}{2}l\langle f(r) \rangle_{nl}, & \text{for } j = l + 1/2, \end{cases} \end{aligned} \quad (10)$$

with  $\langle f(r) \rangle_{nl} \approx -20A^{-2/3}$  and  $\hbar\omega = 45A^{-1/3} - 25A^{-2/3}$ .

The electric transition strength is given by [11]

$$B(CJ, k) = \frac{Z^2}{4\pi} \left[ \frac{(2J+1)!!}{k^J} \right]^2 F_J^2(k), \quad (11)$$

where  $k = E_x/\hbar c$ .

**Table 1.** Theoretical values of the reduced transition probabilities  $B(C4 \uparrow)$  (in units of  $10^3 e^2 \cdot \text{fm}^8$ ) for the transition  $0^+$  to  $4^+$  in comparison with experimental values.

Nucleus	$E_x$ (MeV)	$0\hbar\omega$	$(0+2)\hbar\omega$	$(0+2+4)\hbar\omega$	$sd$ ( $e_p + e_n = 2.0 e$ )	Expt.
$^{20}\text{Ne}$	4.248	11.50	34.10	44.25	46.2	$38 \pm 8^{(a)}$
$^{24}\text{Mg}$	6.010	9.86	30.10	39.31	39.5	$43 \pm 6^{(b)}$
$^{28}\text{Si}$	4.617	6.93	21.83	28.7	27.7	$27.5 \pm 5^{(c)}$
$^{32}\text{S}$	4.459	12.50	39.91	52.8	49.9	$49.9^{(d)}$

(a) Ref. [14].

(b) Ref. [16].

(c) Ref. [18].

(d) Effective charge model [1].

## 1 Results and discussion

The core polarization effects are calculated with the MSDI as a residual interaction. The parameters of the MSDI are denoted by  $A_T$ ,  $B$  and  $C$  [8], where  $T$  indicates the isospin (0,1). An empirical estimate of these parameters can be obtained by comparing the calculated  $B(C4)$  values for even-even *sd*-shell nuclei obtained from the empirical effective charges and those obtained from the core polarization calculations. Based on several experimentally measured transition strengths, the empirical isoscalar  $C4$  effective charge was found to be equal to  $e_p + e_n = (2.0 \pm 0.2)e$  [12]. Using this value for the effective charge, the average value for the strength parameters is found to be equal to  $A0 = A1 = B = 0.42$  MeV and  $C = 0$ . Using this value for the strength parameters, the calculated  $B(C4)$  values are very close to the experimental values as given in table 1.

In all of the following diagrams (see fig. 1), the dashed lines give the results obtained using the *sd*-shell wave functions of Wildenthal interaction [7]. The results of the core polarization effects are shown by the cross symbols. The results including core polarization are shown by the solid lines. For comparisons, we include the results of ref. [1], where the core polarization effects were calculated by assuming a Tassie [13] shape for the core polarization transition density. These results are displayed in the following diagrams by the dotted lines for the core polarization contributions and by the dash-dotted lines for the sum of the model space and core polarization contributions.

### $^{20}\text{Ne}$ nucleus (4.248 MeV, $J^\pi T = 4^+0$ ) state

The *sd*-shell model space ( $0\hbar\omega$ ) calculation predicts the value  $11.5 \times 10^3 e^2 \cdot \text{fm}^8$  for the  $B(C4)$  transition strength when bare charges are used. This value is a factor of more than three lower than the measured value  $(38 \pm 8) \times 10^3 e^2 \cdot \text{fm}^8$  [14] as given in table 1. The  $C4$  form factor according to this model is shown in fig. 1(a) as a dashed curve, where it underpredicts the data. This model cannot reproduce both the transition strength (defined at the photon point) and the non-zero  $q$  values when bare charges are used. Using a  $q$ -independent

effective charge ( $2.0 e$ ) will enhance the photon point and the entire plot by a constant factor and cannot describe the form factor for the different  $q$  regions. The *sd*-shell component represents 26% of the total wave function. When core polarization is included, the particle-hole (ph) component represents 51% with  $2\hbar\omega$  excitations. The  $4\hbar\omega$  contribution is 23% of the total wave function. The core polarization contribution ( $2+4$ )  $\hbar\omega$  represents 74% of the total contribution. This contribution is shown by the cross symbols. The inclusion of this contribution to the model space contribution enhances the form factor for  $q \leq 2.0 \text{ fm}^{-1}$  and describes the experimental data of ref. [15] very well for all  $q$  values as shown by the solid line in fig. 1(a). The core polarization contribution calculated in this work according to the perturbation theory (cross symbols) gives almost an identical result as that obtained by the Tassie shape for the transition density [1] (dotted line) for  $q \leq 2.0 \text{ fm}^{-1}$ . The form factor in this case is given by the dash-dotted line.

### $^{24}\text{Mg}$ nucleus (6.01 MeV, $J^\pi T = 4^+0$ ) state

The predicted  $B(C4)$  value from the *sd*-shell model space calculation with bare charges is  $9.86 \times 10^3 e^2 \cdot \text{fm}^8$ , which is a factor of more than four lower than the measured value  $(43 \pm 6) \times 10^3 e^2 \cdot \text{fm}^8$  [16]. This discrepancy between the experimental and theoretical  $B(C4)$  values is reflected in the form factor, as shown in fig. 1(b) by the dashed curve, where the data is underestimated for  $q \leq 2.0 \text{ fm}^{-1}$ . The inclusion of higher-excited configurations greatly modifies the form factor and shows an excellent agreement with the experimental data of refs. [16,17]. The *sd*-shell component represents 25% of the total wave function. When core polarization is included, the ph component represents 52% with  $2\hbar\omega$  excitations. The  $4\hbar\omega$  contribution is 23% of the total wave function. The core polarization contribution ( $2+4$ )  $\hbar\omega$  represents 75% of the total contribution. This enhancement of the form factor upon the *sd*-shell model form factor was also shown by the projected Hartree-Fock calculation [2], where the numerous small elements beyond the *sd*-shell were important in giving quality of fit to the data.

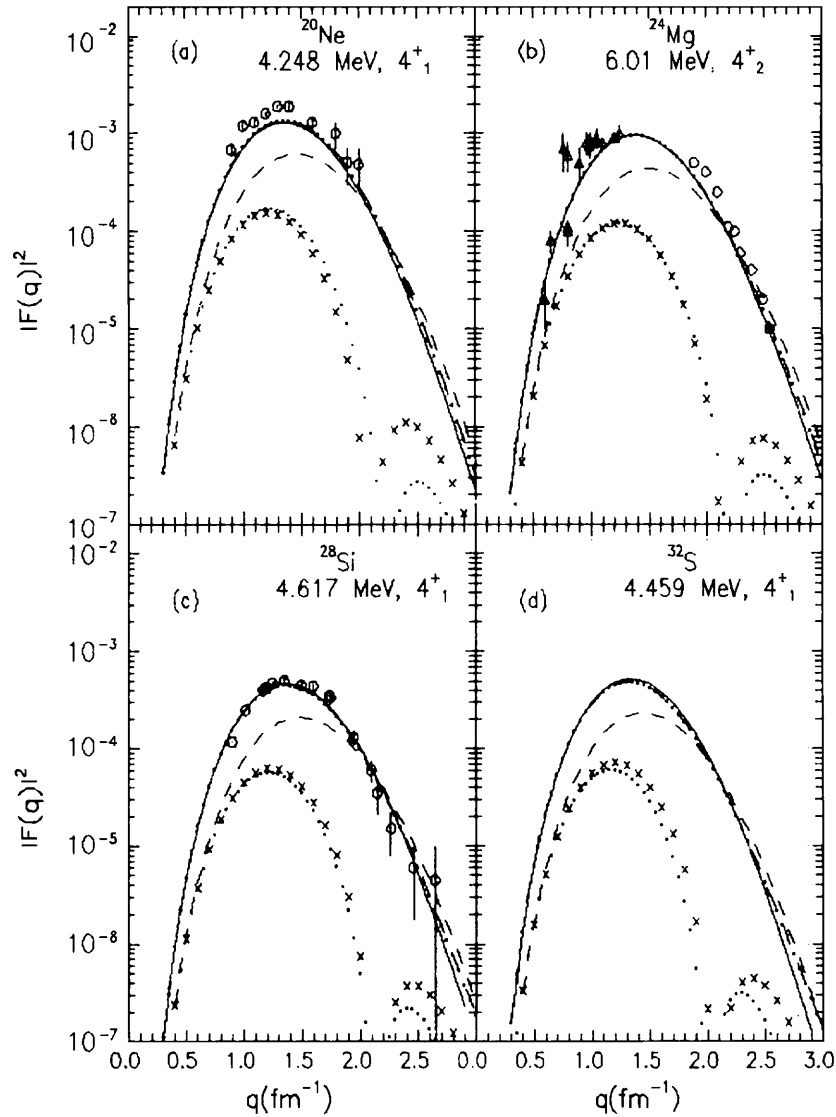


**Fig. 1.** Longitudinal  $C4$  form factors for the transitions to the  $4_1^+$  state in  $^{20}\text{Ne}$  (a), the  $4_2^+$  state in  $^{24}\text{Mg}$  (b), the  $4_1^+$  state in  $^{28}\text{Si}$  (c) and the  $4_1^+$  state in  $^{32}\text{S}$  (d). The dashed lines represents  $sd$ -shell model calculations. Cross symbols represent core polarization contribution. The solid lines represent the sum of  $sd$ -shell and the core polarization contributions. The dotted curves represent the core polarization contribution of ref. [1]. The dash-dotted curves represent the sum of  $sd$ -shell and the core polarization contributions of ref. [1]. The data are taken from ref. [15] for  $^{20}\text{Ne}$ , refs. [16, 17] for  $^{24}\text{Mg}$  and ref. [2] for  $^{28}\text{Si}$ .

### $^{28}\text{Si}$ nucleus (4.62 MeV, $J^\pi T = 4^+0$ ) state

The modification of the  $C4$  form factor by including the core polarization effect upon the  $sd$ -shell model space calculation for  $^{20}\text{Ne}$  and  $^{24}\text{Mg}$  is also noted in  $^{28}\text{Si}$  as shown by the solid line in fig. 1(c) in comparison with the experimental data extracted from ref. [2]. The predicted  $B(C4)$  values for  $sd$ -shell model space with bare charges ( $0\hbar\omega$ ) is  $6.93 \times 10^3 e^2 \cdot \text{fm}^8$  while the inclusion of the core polarization effect gives the value  $28.7 \times 10^3 e^2 \cdot \text{fm}^8$ , in comparison with the experimental result  $(27 \pm 5) \times 10^3 e^2 \cdot \text{fm}^8$  [18] as given in table 1. The  $sd$ -shell component represents 24% of the total wave function. When core polarization is included, the  $ph$  component represents 52% with  $2\hbar\omega$  excitations. The  $4\hbar\omega$  contribution is 24% of the total wave

function. The core polarization contribution ( $2+4$ ) $\hbar\omega$  represents 76% of the total contribution.

### $^{32}\text{S}$ nucleus (4.459) MeV, $J^\pi T = 4^+0$ ) state

The  $sd$ -shell model space calculation ( $0\hbar\omega$ ) predicts the value  $12.5 \times 10^3 e^2 \cdot \text{fm}^8$  for the  $B(C4)$  transition strength. The  $C4$  form factor according to this model is shown in fig. 1(d) as a dashed curve. The core polarization calculations of the higher-excited configurations are shown by the cross symbols. The inclusion of these configurations enhances the form factors for  $q \leq 2.0 \text{ fm}^{-1}$ . No experimental data are available for this nucleus. However, the behavior of the form factor with the inclusion of higher

configurations up to  $4\hbar\omega$  is the same as the previous cases, and gives the same results as those of the Tassie shape for the core polarization transition density [1]. We expect that this model will describe the data when they become available. The calculated transition strength  $B(C4)$  with the inclusion of core polarization effects is  $52.8 \times 10^3 e^2 \cdot \text{fm}^8$ , in comparison with  $49.9 \times 10^3 e^2 \cdot \text{fm}^8$  extracted from the effective charge model [1] as given in table 1. The decomposition of the wave function into *sd* and *ph* components are the same as in  $^{28}\text{Si}$ .

## Conclusions

The *sd*-shell model space wave functions give just around 30% of the total observed *C4* transitions strengths. The inclusion of higher-excited configurations was essential in order to resolve the shortfall. When this was done, by means of core polarization calculation, most of the *C4* strengths were accounted for. The inclusion of core polarization gives a remarkable improvement in the form factors for these nuclei both in the absolute strength and the momentum transfer dependence. The higher  $q$  ( $q > 2.0 \text{ fm}^{-1}$ ) values do not affected by core polarization effects, thus agreed very well with the experimental data. The intermediate states, and hence the  $B(C4)$  values are sensitive to the residual interaction between particles out of the model space. Same strength parameters of the MSDI are used for all nuclei considered in this work which are consistent with the measured form factors both in the absolute strength and the  $q$ -dependence.

## References

1. B.A. Brown, R.A. Radhi, B.H. Wildenthal, Phys. Rep. **101**, 313 (1983).
2. H. Sagawa, B.A. Brown, Phys. Lett. B **150**, 247 (1985).
3. T. Sato, K. Koshigiri, H. Ohtsubo, Z. Phys. A **320**, 507 (1985).
4. T. Sato, N. Odagawa, H. Ohtsubo, T.S.H. Lee, Phys. Rev. C **49**, 776 (1994).
5. A. Cichocki, J. Dubach, R.S. Hicks, G.A. Peterson, C.W. de Jager, H. de Vries, N. Kalantar-Nayestanaki, T. Sato, Phys. Rev. C **51**, 2406 (1995).
6. N. Nose, K. Kume, Phys. Rev. C **54**, 432 (1996).
7. B.H. Wildenthal, Prog. Part. Nucl. Phys. **11**, 5 (1984).
8. P.J. Brussaard, P.W.M. Glaudemans, *Shell Model Applications in Nuclear Spectroscopy* (North-Holland, Amsterdam, 1978).
9. T. deForest jr., J.D. Walecka, Adv. Phys. **15**, 1 (1966).
10. T.W. Donnelly, I. Sick, Rev. Mod. Phys. **56**, 461 (1984).
11. B.A. Brown, B.H. Wildenthal, C.F. Williamson, F.N. Rad, S. Kowalski, H. Cronnel, J.T. O'Brien, Phys. Rev. C **32**, 1127 (1985).
12. B.A. Brown, W. Chung, B.H. Wildenthal, Phys. Rev. C **21**, 2600 (1980).
13. L.J. Tassie, Aust. J. Phys. **9**, 407 (1956).
14. R.P. Singhal *et al.*, Can. J. Phys. **51**, 2125 (1973).
15. Y. Horikawa, Y. Torizuka, A. Nakada, S. Mitsunobu, Y. Kojima, M. Kimura, Phys. Lett. B **36**, 9 (1971).
16. C.G. Li, M.R. Yearian, I. Sick, Phys. Rev. C **9**, 1861 (1974).
17. A. Johnston, T.E. Drake, J. Phys. A **7**, 898 (1974).
18. A. Nakada, Y. Torizuka, J. Phys. Soc. Jpn. **32**, 1 (1972).